COMPDYN 2015
5th ECCOMAS Thematic Conference on
Computational Methods in Structural Dynamics and Earthquake Engineering
M. Papadrakakis, V. Papadopoulos, V. Plevris (eds.)
Crete Island, Greece, 25–27 May 2015

A NEW 3D CO-ROTATIONAL BEAM ELEMENT FOR NONLINEAR DYNAMIC ANALYSIS

Thanh-Nam LE[1,2], Jean-Marc BATTINI [2], and Mohammed HJIAJ[1]

[1]Structural Engineering Research Group - INSA de Rennes
20 Avenue des Buttes de Coësmes, 35708, Rennes, France
{Thanh-Nam.LE, Mohammed.Hjiaj}@insa-rennes.fr

[2] Department of Civil and Architectural Engineering
Royal Institute of Technology, SE-10044 Stockholm, Sweden
jean-marc.battini@byv.kth.se

Keywords: Instructions, ECCOMAS Thematic Conference, Structural Dynamics, Earthquake Engineering, Proceedings.

Abstract. *The paper investigates the contribution of the warping deformations and the shear center location on the dynamic response of 3D thin-walled beams obtained with an original consistent co-rotational formulation developed by the authors. Consistency of the formulation is ensured by employing the same kinematic assumptions to derive both the static and dynamic terms. Hence, the element has seven degrees of freedom at each node and cubic shape functions are used to interpolate local transversal displacements and axial rotations. Accounting for warping deformations and the position of the shear center produces additional terms in the expressions of the inertia force vector and the tangent dynamic matrix. The performance of the present formulation is assessed by comparing its predictions against 3D-solid FE solutions.*

1 INTRODUCTION

The purpose of the present paper is to further develop the dynamic formulation proposed in [31] so that beams with arbitrary thin-walled open cross-sections can be studied. For that, two main ideas are used. Firstly, a seventh degree of freedom is added at each node to describe the warping of the cross-section. Consequently, the linear interpolation for the local axial rotation used in [31] is replaced by a cubic interpolation. Secondly, the main difficulty in the nonlinear analysis of beams with arbitrary cross-sections is that, due to the eccentricity of the shear center, the cross-section rotations are usually not defined at the same point. To avoid this difficulty, the kinematic description proposed by Gruttmann et al. [1] is adopted. In this approach, the warping function is modified and all the cross-section rotations are defined at the centroid.

Consequently, the inertia terms are consistent with the static ones developed by Battini and Pacoste in [5] since the same corotational kinematic description is used to derive all the terms. Regarding the dynamic terms, i.e. the inertia force vector and tangent dynamic matrix, the formulation proposed in [31] is extended and several additional terms are introduced. The contribution of these terms in the performance of the formulation is then investigated in the numerical examples. Regarding the static deformational terms, i.e. the internal force vector and tangent stiffness matrix, the corotational beam element developed by Battini and Pacoste [5] is adopted. However, in order to introduce the bending shear deformations, the cubic Hermitian functions are modified as suggested in the Interdependent Interpolation Element (IIE) formulation [39].

2 PARAMETRIZATION OF FINITE ROTATION

In this section, the basic relations concerning the parameterizations of finite rotations are briefly presented. For a more complete description, the reader is referred to textbooks and review papers such as [2, 12, 16, 20, 21, 28].

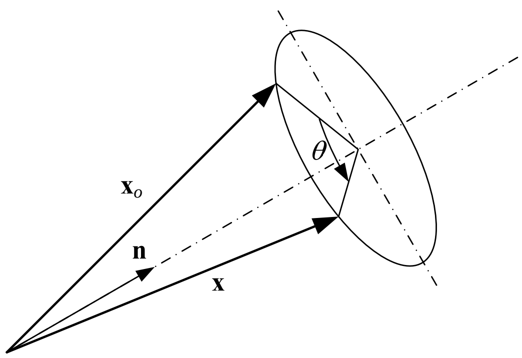

Figure 1: Finite rotation of a vector

The coordinate of a vector $\mathbf{x}_o$ that is rotated into the position $\mathbf{x}$ (see Fig. 1) is given by the relation

$$\mathbf{x} = \mathbf{R}\,\mathbf{x}_o\,. \tag{1}$$

Due to its orthonormality, the rotation matrix $\mathbf{R}$ can be parameterized using only three independent parameters. One possibility is to use the rotational vector defined by

$$\boldsymbol{\theta} = \theta\,\mathbf{n}\,, \tag{2}$$

where $\mathbf{n}$ is a unit vector defining the axis of the rotation and $\theta = (\boldsymbol{\theta}^{\mathrm{T}}\boldsymbol{\theta})^{1/2}$ is the angle of the rotation.

The relation between the rotation matrix and the rotational vector is given by the Rodrigues' formula

$$\mathbf{R} = \mathbf{I} + \frac{\sin\theta}{\theta}\widetilde{\boldsymbol{\theta}} + \frac{1-\cos\theta}{\theta^2}\widetilde{\boldsymbol{\theta}}\,\widetilde{\boldsymbol{\theta}} = \exp(\widetilde{\boldsymbol{\theta}})\,, \tag{3}$$

where $\widetilde{\boldsymbol{\theta}}$ is the skew matrix associated with the vector $\boldsymbol{\theta}$.

The variation of the rotation matrix in spatial and material form is given by

$$\delta\mathbf{R} = \widetilde{\delta\mathbf{w}}\mathbf{R} = \mathbf{R}\widetilde{\delta\boldsymbol{\omega}}\,. \tag{4}$$

Physically, $\widetilde{\delta\mathbf{w}}$ represents infinitesimal spatial rotation superposed onto the rotation $\mathbf{R}$. $\delta\mathbf{w}$, which is also denoted as spatial spin variables, is related to the variation of the rotational vector through

$$\delta\mathbf{w} = \mathbf{T}_s(\boldsymbol{\theta})\,\delta\boldsymbol{\theta}\,, \tag{5}$$

with

$$\mathbf{T}_s(\boldsymbol{\theta}) = \mathbf{I} + \frac{1-\cos\theta}{\theta^2}\widetilde{\boldsymbol{\theta}} + \frac{\theta-\sin\theta}{\theta^3}\widetilde{\boldsymbol{\theta}}\widetilde{\boldsymbol{\theta}}\,. \tag{6}$$

The time derivative of the rotation matrix in spatial and material form is given by

$$\dot{\mathbf{R}} = \widetilde{\dot{\mathbf{w}}}\mathbf{R} = \mathbf{R}\widetilde{\dot{\boldsymbol{\omega}}}\,, \tag{7}$$

where the axis vectors $\dot{\mathbf{w}}$ and $\dot{\boldsymbol{\omega}}$ are spatial and material angular velocities, respectively.

The spatial and material quantities are connected by the relations

$$\delta\mathbf{w} = \mathbf{R}\,\delta\boldsymbol{\omega}\,, \tag{8}$$

$$\dot{\mathbf{w}} = \mathbf{R}\,\dot{\boldsymbol{\omega}}\,, \tag{9}$$

$$\ddot{\mathbf{w}} = \mathbf{R}\,\ddot{\boldsymbol{\omega}}\,. \tag{10}$$

The variation of the material angular velocity is given by (see [8])

$$\delta\dot{\boldsymbol{\omega}} = \dot{\delta\boldsymbol{\omega}} + \widetilde{\dot{\boldsymbol{\omega}}}\,\delta\boldsymbol{\omega}\,, \tag{11}$$

with $\dot{\delta\boldsymbol{\omega}}$ denoting the time derivative of the material spin variables.

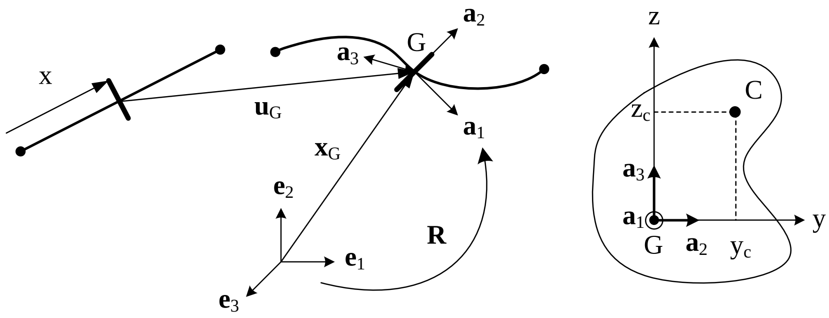

Figure 2: Initial and current configuration of the beam

3 KINETIC ENERGY

In the present paper, the kinematic description proposed by Gruttmann et al. [1] is adopted (see Fig. 2). A beam with an arbitrary cross-section is considered. G and C are the centroid and the shear center of the cross-section. $\mathbf{e}_i$ and $\mathbf{a}_i$ $(i = 1,2,3)$ denote the global and cross-section-attached orthogonal coordinates systems, respectively. The transformation from the global coordinates system to the cross-section-attached one is defined by

$$\mathbf{a}_i = \mathbf{R}\,\mathbf{e}_i\,. \tag{12}$$

Let $\mathbf{x}_{\mathrm{P}}(x,y,z)$ denote the position vector of an arbitrary point P in the current configuration

$$\mathbf{x}_{\mathrm{P}}(x,y,z) = \mathbf{x}_{\mathrm{G}}(x) + y\,\mathbf{a}_2(x) + z\,\mathbf{a}_3(x) + \alpha(x)\,\overline{\omega}(y,z)\,\mathbf{a}_1(x)\,, \tag{13}$$

with $\mathbf{x}_{\mathrm{G}}$ denoting the position vector of G in the current configuration.

The warping function $\overline{\omega}(y,z)$ is defined within the Saint-Venant torsion theory and refers to the centroid G, i.e.

$$\overline{\omega} = \omega - y_c\,z + z_c\,y\,, \tag{14}$$

where ω refers to the shear center C with coordinates $y_c\,,z_c$. Note that in connection with ω, the following normality conditions hold

$$\int_A \omega\,\mathrm{d}A = 0\,, \quad \int_A \omega\,y\,\mathrm{d}A = 0\,, \quad \int_A \omega\,z\,\mathrm{d}A = 0\,. \tag{15}$$

Using Eq. (12), the expression (13) can be put in the form

$$\mathbf{x}_{\mathrm{P}} = \mathbf{x}_{\mathrm{G}} + \mathbf{R}\,(\mathbf{X} + \alpha\,\mathbf{n}_{\overline{\omega}})\,, \tag{16}$$

with $\mathbf{X} = [0\;\;y\;\;z]^{\mathrm{T}}$ and $\mathbf{n}_{\overline{\omega}} = [\overline{\omega}\;\;0\;\;0]^{\mathrm{T}}$.

By taking the time derivative of the above expression and using Eq. (7), the velocity is obtained as

$$\begin{aligned}\dot{\mathbf{u}}_{\mathrm{P}} = \dot{\mathbf{x}}_{\mathrm{P}} &= \dot{\mathbf{x}}_{\mathrm{G}} + \mathbf{R}\,\widetilde{\dot{\boldsymbol{\omega}}}(\mathbf{X} + \alpha\,\mathbf{n}_{\overline{\omega}}) + \mathbf{R}\,\dot{\alpha}\,\mathbf{n}_{\overline{\omega}} \\ &= \dot{\mathbf{u}}_{\mathrm{G}} + \mathbf{R}\,(-\widetilde{\mathbf{X}}\,\dot{\boldsymbol{\omega}} - \alpha\,\widetilde{\mathbf{n}_{\overline{\omega}}}\,\dot{\boldsymbol{\omega}} + \dot{\alpha}\,\mathbf{n}_{\overline{\omega}})\,.\end{aligned} \tag{17}$$

The kinetic energy of the beam is then calculated by

$$K = \frac{1}{2}\int_V \rho\, \dot{\mathbf{u}}_{\mathrm{P}}^{\mathrm{T}}\, \dot{\mathbf{u}}_{\mathrm{P}}\ \mathrm{d}V = \frac{1}{2}\Bigg[\int_{l_o} \dot{\mathbf{u}}_{\mathrm{G}}^{\mathrm{T}}\, A_\rho\, \dot{\mathbf{u}}_{\mathrm{G}}\ \mathrm{d}l + \int_V \rho\, (-\widetilde{\mathbf{X}}\,\dot{\boldsymbol{\omega}} - \alpha\,\widetilde{\mathbf{n}_{\overline{\omega}}}\,\dot{\boldsymbol{\omega}} + \dot{\alpha}\,\mathbf{n}_{\overline{\omega}})^{\mathrm{T}}\, (-\widetilde{\mathbf{X}}\,\dot{\boldsymbol{\omega}} - \alpha\,\widetilde{\mathbf{n}_{\overline{\omega}}}\,\dot{\boldsymbol{\omega}} + \dot{\alpha}\,\mathbf{n}_{\overline{\omega}})\ \mathrm{d}V\Bigg]. \tag{18}$$

The following notations are introduced

$$I_{yz} = \int_A y\,z\,\mathrm{d}A\,,\quad I_{yy} = \int_A y^2\,\mathrm{d}A\,,\quad I_{zz} = \int_A z^2\,\mathrm{d}A\,,\quad I_\omega = \int_A \omega^2\,\mathrm{d}A\,, \tag{19}$$

$$I_{\overline{\omega}} = \int_A \overline{\omega}^2\,\mathrm{d}A = I_\omega + z_c^2\,I_{yy} + y_c^2\,I_{zz} - 2\,y_c\,z_c\,I_{yz}\,, \tag{20}$$

$$I_{yc} = \int_A y\,\overline{\omega}\,\mathrm{d}A = -y_c\,I_{yz} + z_c\,I_{yy}\,, \tag{21}$$

$$I_{zc} = \int_A z\,\overline{\omega}\,\mathrm{d}A = -y_c\,I_{zz} + z_c\,I_{yz}\,, \tag{22}$$

$$\mathbf{J}_\rho = \int_A \rho\,\widetilde{\mathbf{X}}^{\mathrm{T}}\,\widetilde{\mathbf{X}}\ \mathrm{d}A = \rho\begin{bmatrix} I_{yy}+I_{zz} & 0 & 0 \\ 0 & I_{zz} & -I_{yz} \\ 0 & -I_{yz} & I_{yy} \end{bmatrix}, \tag{23}$$

$$\mathbf{J}_{\overline{\omega}} = \int_A \rho\,\widetilde{\mathbf{n}_{\overline{\omega}}}^{\mathrm{T}}\,\widetilde{\mathbf{n}_{\overline{\omega}}}\ \mathrm{d}A = \rho\begin{bmatrix} 0 & 0 & 0 \\ 0 & I_{\overline{\omega}} & 0 \\ 0 & 0 & I_{\overline{\omega}} \end{bmatrix}, \tag{24}$$

$$\mathbf{J}_a = \int_A \rho\,\left(\widetilde{\mathbf{X}}^{\mathrm{T}}\,\widetilde{\mathbf{n}_{\overline{\omega}}} + \widetilde{\mathbf{n}_{\overline{\omega}}}^{\mathrm{T}}\,\widetilde{\mathbf{X}}\right)\ \mathrm{d}A = \rho\begin{bmatrix} 0 & -I_{yc} & -I_{zc} \\ -I_{yc} & 0 & 0 \\ -I_{zc} & 0 & 0 \end{bmatrix}, \tag{25}$$

$$\mathbf{J}_b = \int_A \rho\,\widetilde{\mathbf{X}}^{\mathrm{T}}\,\mathbf{n}_{\overline{\omega}}\ \mathrm{d}A = \rho\begin{bmatrix} 0 \\ -I_{zc} \\ I_{yc} \end{bmatrix}, \tag{26}$$

$$\mathbf{J}_\alpha = \alpha^2\,\mathbf{J}_{\overline{\omega}} + \alpha\,\mathbf{J}_a\,,\quad J_{\overline{\omega}} = \rho\,I_{\overline{\omega}}\,. \tag{27}$$

The expression of the kinetic energy can then be rewritten in the material form as

$$K = \frac{1}{2}\int_{l_o}\left[\dot{\mathbf{u}}_{\mathrm{G}}^{\mathrm{T}}\,A_\rho\,\dot{\mathbf{u}}_{\mathrm{G}} + \dot{\boldsymbol{\omega}}^{\mathrm{T}}\,\mathbf{J}_\rho\,\dot{\boldsymbol{\omega}}\right]\ \mathrm{d}l + \frac{1}{2}\int_{l_o}\left[\dot{\boldsymbol{\omega}}^{\mathrm{T}}\,\mathbf{J}_\alpha\,\dot{\boldsymbol{\omega}} - 2\,\dot{\boldsymbol{\omega}}^{\mathrm{T}}\,\mathbf{J}_b\,\dot{\alpha} + J_{\overline{\omega}}\,\dot{\alpha}^2\right]\ \mathrm{d}l\,, \tag{28}$$

and, using Eq. (9), the spatial form is obtained

$$K = \frac{1}{2}\int_{l_o}\left[\dot{\mathbf{u}}_{\mathrm{G}}^{\mathrm{T}}\,A_\rho\,\dot{\mathbf{u}}_{\mathrm{G}} + \dot{\mathbf{w}}^{\mathrm{T}}\,\mathbf{I}_\rho\,\dot{\mathbf{w}}\right]\ \mathrm{d}l + \frac{1}{2}\int_{l_o}\left[\dot{\mathbf{w}}^{\mathrm{T}}\,\mathbf{I}_\alpha\,\dot{\mathbf{w}} - 2\,\dot{\mathbf{w}}^{\mathrm{T}}\,\mathbf{I}_b\,\dot{\alpha} + J_{\overline{\omega}}\,\dot{\alpha}^2\right]\ \mathrm{d}l\,, \tag{29}$$

with

$$\mathbf{I}_\rho = \mathbf{R}\,\mathbf{J}_\rho\,\mathbf{R}^{\mathrm{T}}\,,\quad \mathbf{I}_{\overline{\omega}} = \mathbf{R}\,\mathbf{J}_{\overline{\omega}}\,\mathbf{R}^{\mathrm{T}}\,,\quad \mathbf{I}_\alpha = \mathbf{R}\,\mathbf{J}_\alpha\,\mathbf{R}^{\mathrm{T}}\,,\quad \mathbf{I}_b = \mathbf{R}\,\mathbf{J}_b\,. \tag{30}$$

The first integrals in Eqs. (28) and (29) are the kinetic energy due to the translation and rotation of the beam cross-section. The variation, in the spatial form, is obtained as

$$\delta K_{Trans+Rot} = -\int_{l_o} \left\{ \delta \mathbf{u}_{\mathrm{G}}{}^{\mathrm{T}} A_\rho \ddot{\mathbf{u}}_{\mathrm{G}} + \delta \mathbf{w}^{\mathrm{T}} \left[\mathbf{I}_\rho \ddot{\mathbf{w}} + \widetilde{\dot{\mathbf{w}}} \mathbf{I}_\rho \dot{\mathbf{w}} \right] \right\} \mathrm{d}l \,. \tag{31}$$

The second integrals in Eqs. (28) and (29), named as $K_{Warping}$, are the additional kinetic energy due to the warping deformations and the eccentricity of shear center with respect to the centroid

$$K_{Warping} = \int_{l_o} k_W \;\; \mathrm{d}l = \frac{1}{2} \int_{l_o} \left[\dot{\boldsymbol{\omega}}^{\mathrm{T}} \, \mathbf{J}_\alpha \, \dot{\boldsymbol{\omega}} - 2 \, \dot{\boldsymbol{\omega}}^{\mathrm{T}} \, \mathbf{J}_b \, \dot{\alpha} + J_{\overline{\omega}} \, \dot{\alpha}^2 \right] \;\; \mathrm{d}l \,. \tag{32}$$

The variation of k_W is given by

$$\delta k_W = \delta \dot{\boldsymbol{\omega}}^{\mathrm{T}} \; (\mathbf{J}_\alpha \, \dot{\boldsymbol{\omega}} - \mathbf{J}_b \, \dot{\alpha}) + \delta \alpha \, \dot{\boldsymbol{\omega}}^{\mathrm{T}} \, \mathbf{J}_\alpha^{'} \, \dot{\boldsymbol{\omega}} + \delta \dot{\alpha} \; (J_{\overline{\omega}} \, \dot{\alpha} - \dot{\boldsymbol{\omega}}^{\mathrm{T}} \, \mathbf{J}_b) \,, \tag{33}$$

where

$$\mathbf{J}_\alpha^{'} = \frac{1}{2} \frac{\mathrm{d}\mathbf{J}_\alpha}{\mathrm{d}\alpha} = \alpha \, \mathbf{J}_{\overline{\omega}} + \frac{1}{2} \, \mathbf{J}_a \,. \tag{34}$$

In order to derive an expression which only depends on infinitesimal rotations, an integration in time is performed using Eqs. (11) and (33)

$$\begin{aligned} \int_{t_1}^{t_2} \delta k_W \mathrm{d}t = & \int_{t_1}^{t_2} \dot{\delta \boldsymbol{\omega}}^{\mathrm{T}} \; (\mathbf{J}_\alpha \, \dot{\boldsymbol{\omega}} - \mathbf{J}_b \, \dot{\alpha}) \; \mathrm{d}t + \int_{t_1}^{t_2} \delta \boldsymbol{\omega}^{\mathrm{T}} \, \widetilde{\dot{\boldsymbol{\omega}}}^{\mathrm{T}} \; (\mathbf{J}_\alpha \, \dot{\boldsymbol{\omega}} - \mathbf{J}_b \, \dot{\alpha}) \; \mathrm{d}t \\ & + \int_{t_1}^{t_2} \delta \alpha \, \dot{\boldsymbol{\omega}}^{\mathrm{T}} \, \mathbf{J}_\alpha^{'} \, \dot{\boldsymbol{\omega}} \; \mathrm{d}t + \int_{t_1}^{t_2} \delta \dot{\alpha} \; (J_{\overline{\omega}} \, \dot{\alpha} - \dot{\boldsymbol{\omega}}^{\mathrm{T}} \, \mathbf{J}_b) \; \mathrm{d}t \,. \end{aligned} \tag{35}$$

The first and fourth terms in the above expression are integrated by parts

$$\begin{aligned} \int_{t_1}^{t_2} \dot{\delta \boldsymbol{\omega}}^{\mathrm{T}} \; (\mathbf{J}_\alpha \, \dot{\boldsymbol{\omega}} - \mathbf{J}_b \, \dot{\alpha}) \; \mathrm{d}t = & \; \delta \boldsymbol{\omega}^{\mathrm{T}} \; (\mathbf{J}_\alpha \, \dot{\boldsymbol{\omega}} - \mathbf{J}_b \, \dot{\alpha}) \Big|_{t_1}^{t_2} \\ & - \int_{t_1}^{t_2} \delta \boldsymbol{\omega}^{\mathrm{T}} \; (\mathbf{J}_\alpha \, \ddot{\boldsymbol{\omega}} - \mathbf{J}_b \, \ddot{\alpha}) \; \mathrm{d}t - \int_{t_1}^{t_2} \delta \boldsymbol{\omega}^{\mathrm{T}} \, 2 \, \mathbf{J}_\alpha^{'} \, \dot{\alpha} \, \dot{\boldsymbol{\omega}} \; \mathrm{d}t \,, \end{aligned} \tag{36}$$

$$\int_{t_1}^{t_2} \delta \dot{\alpha} \; (J_{\overline{\omega}} \, \dot{\alpha} - \dot{\boldsymbol{\omega}}^{\mathrm{T}} \, \mathbf{J}_b) \; \mathrm{d}t = \delta \alpha (J_{\overline{\omega}} \, \dot{\alpha} - \dot{\boldsymbol{\omega}}^{\mathrm{T}} \, \mathbf{J}_b) \Big|_{t_1}^{t_2} - \int_{t_1}^{t_2} \delta \alpha \; (J_{\overline{\omega}} \, \ddot{\alpha} - \ddot{\boldsymbol{\omega}}^{\mathrm{T}} \, \mathbf{J}_b) \; \mathrm{d}t \,. \tag{37}$$

Due to the arbitrariness of the variations $\delta \boldsymbol{\omega}$ and $\delta \alpha$

$$\delta \boldsymbol{\omega}^{\mathrm{T}} \; (\mathbf{J}_\alpha \, \dot{\boldsymbol{\omega}} - \mathbf{J}_b \, \dot{\alpha}) \Big|_{t_1}^{t_2} = 0 \,, \tag{38}$$

$$\delta \alpha (J_{\overline{\omega}} \, \dot{\alpha} - \dot{\boldsymbol{\omega}}^{\mathrm{T}} \, \mathbf{J}_b) \Big|_{t_1}^{t_2} = 0 \,, \tag{39}$$

hence, using Eqs. (36) and (37), Eq. (33) can be rewritten as

$$\delta k_W = - \begin{bmatrix} \delta \boldsymbol{\omega} \\ \delta \alpha \end{bmatrix}^{\mathrm{T}} \begin{bmatrix} \mathbf{J}_\alpha & -\mathbf{J}_b \\ -\mathbf{J}_b^{\mathrm{T}} & J_{\overline{\omega}} \end{bmatrix} \begin{bmatrix} \ddot{\boldsymbol{\omega}} \\ \ddot{\alpha} \end{bmatrix} - \begin{bmatrix} \delta \boldsymbol{\omega} \\ \delta \alpha \end{bmatrix}^{\mathrm{T}} \begin{bmatrix} \widetilde{\dot{\boldsymbol{\omega}}} \, \mathbf{J}_\alpha & \mathbf{J}_c \, \dot{\boldsymbol{\omega}} \\ -\dot{\boldsymbol{\omega}}^{\mathrm{T}} \, \mathbf{J}_\alpha^{'} & 0 \end{bmatrix} \begin{bmatrix} \dot{\boldsymbol{\omega}} \\ \dot{\alpha} \end{bmatrix} , \tag{40}$$

where $\mathbf{J}_c = 2\,\mathbf{J}_\alpha^{'} + \widetilde{\mathbf{J}}_b$.

Finally, the variation of the total kinetic energy, in the spatial form, is expressed as

$$\delta K = -\int_{l_o} \left\{ \delta \mathbf{u}_{\mathrm{G}}{}^{\mathrm{T}} A_\rho \ddot{\mathbf{u}}_{\mathrm{G}} + \delta \mathbf{w}^{\mathrm{T}} \left[\mathbf{I}_\rho \ddot{\mathbf{w}} + \widetilde{\dot{\mathbf{w}}} \mathbf{I}_\rho \dot{\mathbf{w}} \right] \right\} \mathrm{d}l - \tag{41}$$

$$\int_{l_o} \begin{bmatrix} \delta \mathbf{w} \\ \delta \alpha \end{bmatrix}^{\mathrm{T}} \begin{bmatrix} \mathbf{I}_\alpha & -\mathbf{I}_b \\ -\mathbf{I}_b^{\mathrm{T}} & J_{\overline{\omega}} \end{bmatrix} \begin{bmatrix} \ddot{\mathbf{w}} \\ \ddot{\alpha} \end{bmatrix} \mathrm{d}l - \int_{l_o} \begin{bmatrix} \delta \mathbf{w} \\ \delta \alpha \end{bmatrix}^{\mathrm{T}} \begin{bmatrix} \widetilde{\dot{\mathbf{w}}}\, \mathbf{I}_\alpha & \mathbf{I}_c\, \dot{\mathbf{w}} \\ -\dot{\mathbf{w}}^{\mathrm{T}}\, \mathbf{I}_\alpha^{'} & 0 \end{bmatrix} \begin{bmatrix} \dot{\mathbf{w}} \\ \dot{\alpha} \end{bmatrix} \mathrm{d}l\,,$$

where $\mathbf{I}_\alpha^{'} = \mathbf{R}\,\mathbf{J}_\alpha^{'}\,\mathbf{R}^{\mathrm{T}}$ and $\mathbf{I}_c = \mathbf{R}\,\mathbf{J}_c\,\mathbf{R}^{\mathrm{T}}$.

By introducing the following notations

$$\delta \mathbf{w}^w = \begin{bmatrix} \delta \mathbf{w} \\ \delta \alpha \end{bmatrix}, \quad \dot{\mathbf{w}}^w = \begin{bmatrix} \dot{\mathbf{w}} \\ \dot{\alpha} \end{bmatrix}, \quad \ddot{\mathbf{w}}^w = \begin{bmatrix} \ddot{\mathbf{w}} \\ \ddot{\alpha} \end{bmatrix}, \tag{42}$$

$$\mathbf{I}_\rho^1 = \begin{bmatrix} (\mathbf{I}_\rho + \mathbf{I}_\alpha) & -\mathbf{I}_b \\ -\mathbf{I}_b^{\mathrm{T}} & J_{\overline{\omega}} \end{bmatrix}, \quad \mathbf{I}_\rho^2 = \begin{bmatrix} \widetilde{\dot{\mathbf{w}}}\,(\mathbf{I}_\rho + \mathbf{I}_\alpha) & \mathbf{I}_c\, \dot{\mathbf{w}} \\ -\dot{\mathbf{w}}^{\mathrm{T}}\, \mathbf{I}_\alpha^{'} & 0 \end{bmatrix}, \tag{43}$$

the expression in Eq. (41) can be put in the form

$$\delta K = -\int_{l_o} \left\{ \delta \mathbf{u}_{\mathrm{G}}{}^{\mathrm{T}} A_\rho \ddot{\mathbf{u}}_{\mathrm{G}} + \delta \mathbf{w}^{w\mathrm{T}} \left[\mathbf{I}_\rho^1 \ddot{\mathbf{w}}^w + \mathbf{I}_\rho^2 \dot{\mathbf{w}}^w \right] \right\} \mathrm{d}l\,. \tag{44}$$

4 BEAM KINEMATICS

In this work, the corotational framework introduced by Rankin and Nour-Omid [36,38], and further developed Battini and Pacoste [5] is fully adopted.

The definition of the corotational two noded-beam element, described in this section, involves several coordinate systems, see Fig. 3. First a global reference system is defined by the triad of unit orthogonal vectors $\mathbf{e}_j$ $(j = 1,2,3)$. Next, a local system which continuously rotates and translates with the element is selected. The orthonormal basis vectors of the local system are denoted by $\mathbf{r}_j$ $(j = 1,2,3)$. In the initial (undeformed) configuration, the local system is defined by the orthonormal triad $\mathbf{e}_j^o$. In addition, $\mathbf{t}_j^1$ and $\mathbf{t}_j^2$ $(j = 1,2,3)$, denote two unit triads rigidly attached to nodes 1 and 2. The origin of each unit triad (except the global one $\mathbf{e}_j$) coincides with the centroid of the cross-section.

According to the main idea of the corotational formulation, the motion of the element from the initial to the final deformed configuration is split into a rigid body component and a deformational part. The rigid body motion consists of a rigid translation and rotation of the local element frame. The origin of the local system is taken at node 1 and thus the rigid translation is defined by $\mathbf{u}_1^g$, the translation of the cross-section centroid at node 1. Here and in the sequel, superscript g indicates quantities expressed in the global reference system. The rigid rotation is such that the new orientation of the local reference system is defined by an orthogonal matrix $\mathbf{R}_r$, given by

$$\mathbf{R}_r = [\,\mathbf{r}_1\;\mathbf{r}_2\;\mathbf{r}_3\,]\,. \tag{45}$$

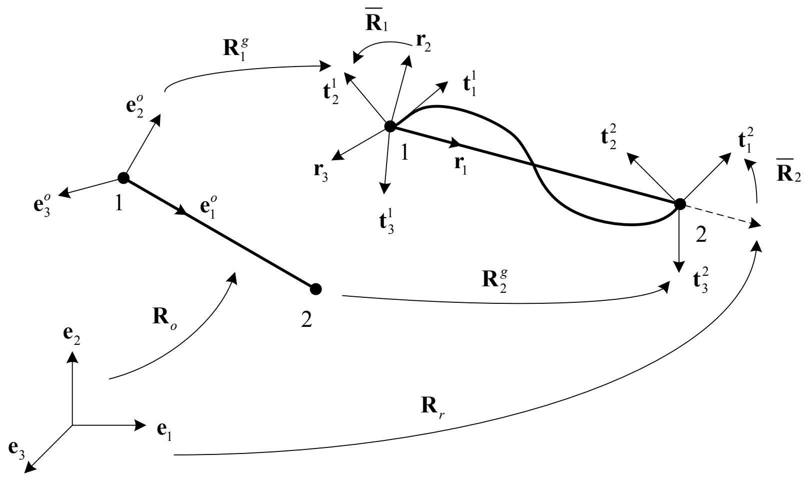

Figure 3: Beam kinematics and the coordinate systems

The first coordinate axis of the local system is defined by the line connecting nodes 1 and 2 of the element. Consequently, $\mathbf{r}_1$ is given by

$$\mathbf{r}_1 = \frac{\mathbf{x}_2^g + \mathbf{u}_2^g - \mathbf{x}_1^g - \mathbf{u}_1^g}{l_n}, \tag{46}$$

with $\mathbf{x}_i^g$ $(i = 1, 2)$ denoting the nodal coordinates in the initial undeformed configuration and l_n denoting the current length of the beam, i.e.

$$l_n = \|\mathbf{x}_2^g + \mathbf{u}_2^g - \mathbf{x}_1^g - \mathbf{u}_1^g\|. \tag{47}$$

The remaining two axes are determined with the help of an auxiliary vector $\mathbf{p}$. In the initial configuration, $\mathbf{p}$ is directed along the local $\mathbf{e}_2^o$ direction, whereas in the deformed configuration its orientation is obtained from

$$\mathbf{p} = \frac{1}{2}(\mathbf{p}_1 + \mathbf{p}_2), \quad \mathbf{p}_i = \mathbf{R}_i^g \mathbf{R}_o [0\ 1\ 0]^{\mathrm{T}} \quad (i = 1, 2), \tag{48}$$

where $\mathbf{R}_1^g$ and $\mathbf{R}_2^g$ are the orthogonal matrices used to specify the orientation of the nodal triads $\mathbf{t}_j^1$ and $\mathbf{t}_j^2$ respectively, and $\mathbf{R}_o$ specifies the orientation of the local frame in the initial configuration, i.e. $\mathbf{R}_o = [\mathbf{e}_1^o\ \mathbf{e}_2^o\ \mathbf{e}_3^o]$. The unit vectors $\mathbf{r}_2$ and $\mathbf{r}_3$ are then computed by the following vector products

$$\mathbf{r}_3 = \frac{\mathbf{r}_1 \times \mathbf{p}}{\|\mathbf{r}_1 \times \mathbf{p}\|}, \quad \mathbf{r}_2 = \mathbf{r}_3 \times \mathbf{r}_1, \tag{49}$$

resulting in the orthogonal matrix $\mathbf{R}_r$ (Eq. (45)) being completely determined.

The rigid motion previously described, is accompanied by local deformational displacements and rotations with respect to the local element axes. In this context, due to the particular choice of the local system, the local translations at node 1 are zero. Moreover, at node 2, the only non zero component is the translation along $\mathbf{r}_1$. This can easily be evaluated according to

$$\bar{u} = l_n - l_o, \tag{50}$$

with l_o denoting the length of the beam in the original undeformed configuration. Here and in the sequel, an overbar denotes a deformational kinematic quantity.

The global rotations at node i can be expressed in terms of the rigid rotation of the local axes, defined by $\mathbf{R}_r$, followed by a local rotation relative to these axes. The latter is defined by the orthogonal matrix $\overline{\mathbf{R}}_i$. Consequently, the orientation of the nodal triad $\mathbf{t}^i_j$ can be obtained by means of the product $\mathbf{R}_r \overline{\mathbf{R}}_i$. On the other hand, (see Fig. 3) this orientation can also be obtained through the product $\mathbf{R}^g_i \mathbf{R}_o$, which gives

$$\overline{\mathbf{R}}_i = \mathbf{R}_r^{\mathrm{T}} \mathbf{R}^g_i \mathbf{R}_o \quad (i = 1,2)\,. \tag{51}$$

The local rotations are then evaluated from

$$\bar{\boldsymbol{\theta}}_i = \log\left(\overline{\mathbf{R}}_i\right) \quad (i = 1,2)\,. \tag{52}$$

Due to the choice of the local coordinate system, the local nodal displacement vector $\mathbf{d}^w_l$ has only nine components and is given by

$$\mathbf{d}^w_l = \left[\bar{u}\ \bar{\boldsymbol{\theta}}_1^{\mathrm{T}}\ \bar{\boldsymbol{\theta}}_2^{\mathrm{T}}\ \alpha_1\ \alpha_2\right]^{\mathrm{T}}. \tag{53}$$

with α_i $(i = 1,2)$ denoting the additional warping degrees of freedom.

The variation of the local nodal displacement vector is

$$\delta\mathbf{d}^w_l = \left[\delta\bar{u}\ \delta\bar{\boldsymbol{\theta}}_1^{\mathrm{T}}\ \delta\bar{\boldsymbol{\theta}}_2^{\mathrm{T}}\ \delta\alpha_1\ \delta\alpha_2\right]^{\mathrm{T}}, \tag{54}$$

and the global counterpart is given by

$$\delta\mathbf{d}^w_g = \left[\delta\mathbf{u}_1^{g\mathrm{T}}\ \delta\mathbf{w}_1^{g\mathrm{T}}\ \delta\mathbf{u}_2^{g\mathrm{T}}\ \delta\mathbf{w}_2^{g\mathrm{T}}\ \delta\alpha_1\ \delta\alpha_2\right]^{\mathrm{T}}, \tag{55}$$

with $\delta\mathbf{w}^g_i$ $(i = 1,2)$ denoting spatial spin variables defined by

$$\delta\mathbf{R}^g_i = \widetilde{\delta\mathbf{w}^g_i}\,\mathbf{R}^g_i\,. \tag{56}$$

Since the warping is a deformational quantity, it remains constant during the transformation between the global and local system, see Eqs. (54) and (55).

Further, let $\delta\overline{\mathbf{w}}_i$ and $\delta\mathbf{w}^g_r$ denote the spatial spin variables defined by

$$\delta\overline{\mathbf{R}}_i = \widetilde{\delta\overline{\mathbf{w}}_i}\,\overline{\mathbf{R}}_i, \quad \delta\mathbf{R}_r = \widetilde{\delta\mathbf{w}^g_r}\,\mathbf{R}_r\,. \tag{57}$$

By taking the variation of Eq. (51), one obtains the following relation (see [5])

$$\delta\overline{\mathbf{w}}_i = \delta\mathbf{w}^e_i - \delta\mathbf{w}^e_r \quad (i = 1,2)\,, \tag{58}$$

where use of Eq. (51) has been made along the fact that $\mathbf{R}_r$ transforms a vector and a tensor from global to local coordinates according to

$$\mathbf{x}^e = \mathbf{R}_r^{\mathrm{T}} \mathbf{x}^g, \quad \widetilde{\mathbf{x}^e} = \mathbf{R}_r^{\mathrm{T}}\, \widetilde{\mathbf{x}^g}\, \mathbf{R}_r\,. \tag{59}$$

Let consider only the global translational and rotational variables

$$\delta\mathbf{d}_g = \left[\delta\mathbf{u}_1^{g\mathrm{T}} \;\; \delta\mathbf{w}_1^{g\mathrm{T}} \;\; \delta\mathbf{u}_2^{g\mathrm{T}} \;\; \delta\mathbf{w}_2^{g\mathrm{T}} \right]^{\mathrm{T}}, \tag{60}$$

and let

$$\delta\mathbf{d}_g^e = \mathbf{E}^{\mathrm{T}}\,\delta\mathbf{d}_g, \quad \mathbf{E} = \begin{bmatrix} \mathbf{R}_r & \mathbf{0} & \mathbf{0} & \mathbf{0} \\ \mathbf{0} & \mathbf{R}_r & \mathbf{0} & \mathbf{0} \\ \mathbf{0} & \mathbf{0} & \mathbf{R}_r & \mathbf{0} \\ \mathbf{0} & \mathbf{0} & \mathbf{0} & \mathbf{R}_r \end{bmatrix}, \tag{61}$$

with $\mathbf{0}$ denoting the 3×3 zero matrix.

Using the chain rule, $\delta\overline{\mathbf{w}}_i$ is evaluated as

$$\delta\overline{\mathbf{w}}_i = \frac{\partial\overline{\mathbf{w}}_i}{\partial\mathbf{d}_g^e}\frac{\partial\mathbf{d}_g^e}{\partial\mathbf{d}_g}\,\delta\mathbf{d}_g = \frac{\partial\overline{\mathbf{w}}_i}{\partial\mathbf{d}_g^e}\,\mathbf{E}^{\mathrm{T}}\,\delta\mathbf{d}_g \quad (i = 1,2). \tag{62}$$

Then Eq. (58) can be rewritten as

$$\begin{bmatrix} \delta\overline{\mathbf{w}}_1 \\ \delta\overline{\mathbf{w}}_2 \end{bmatrix} = \left(\begin{bmatrix} \mathbf{0} & \mathbf{I} & \mathbf{0} & \mathbf{0} \\ \mathbf{0} & \mathbf{0} & \mathbf{0} & \mathbf{I} \end{bmatrix} - \begin{bmatrix} \mathbf{G}^{\mathrm{T}} \\ \mathbf{G}^{\mathrm{T}} \end{bmatrix} \right) \mathbf{E}^{\mathrm{T}}\,\delta\mathbf{d}_g = \mathbf{P}\mathbf{E}^{\mathrm{T}}\,\delta\mathbf{d}_g\,, \tag{63}$$

where the matrix $\mathbf{G}$ is defined by

$$\mathbf{G}^{\mathrm{T}} = \frac{\partial\mathbf{w}_r^e}{\partial\mathbf{d}_g^e}\,. \tag{64}$$

For the local coordinate system defined in Eqs. (46) - (49), the above equation yield to

$$\mathbf{G}^{\mathrm{T}} = \begin{bmatrix} 0 & 0 & \dfrac{\eta}{l_n} & \dfrac{\eta_{12}}{2} & -\dfrac{\eta_{11}}{2} & 0 & 0 & 0 & -\dfrac{\eta}{l_n} & \dfrac{\eta_{22}}{2} & -\dfrac{\eta_{21}}{2} & 0 \\ 0 & 0 & \dfrac{1}{l_n} & 0 & 0 & 0 & 0 & 0 & -\dfrac{1}{l_n} & 0 & 0 & 0 \\ 0 & -\dfrac{1}{l_n} & 0 & 0 & 0 & 0 & 0 & \dfrac{1}{l_n} & 0 & 0 & 0 & 0 \end{bmatrix}, \tag{65}$$

$$\eta = \frac{p_1}{p_2}, \quad \eta_{11} = \frac{p_{11}}{p_2}, \quad \eta_{12} = \frac{p_{12}}{p_2}, \quad \eta_{21} = \frac{p_{21}}{p_2}, \quad \eta_{22} = \frac{p_{22}}{p_2}, \tag{66}$$

where (see Eq. (48)) p_j and p_{ij} are the components of the vectors $\mathbf{R}_r^{\mathrm{T}}\,\mathbf{p}$ and $\mathbf{R}_r^{\mathrm{T}}\,\mathbf{p}_i$, respectively.

5 INERTIA FORCE AND TANGENT DYNAMIC MATRIX

5.1 Local beam kinematic description

The local motion of a beam cross-section from the initial (i.e. rotated but still undeformed) configuration to the current configuration is defined by $[\overline{u}_1 \;\; \overline{u}_2 \;\; \overline{u}_3]^{\mathrm{T}}$, the translation of the cross-section centroid G and $\overline{\boldsymbol{\theta}} = [\overline{\theta}_1 \;\; \overline{\theta}_2 \;\; \overline{\theta}_3]^{\mathrm{T}}$, the local rotation of the section (see Figs. 4 and 5) and α, the warping intensity (see Eq. (13)).

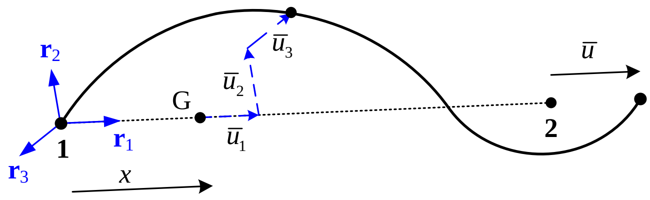

Figure 4: Local beam configuration - Translation.

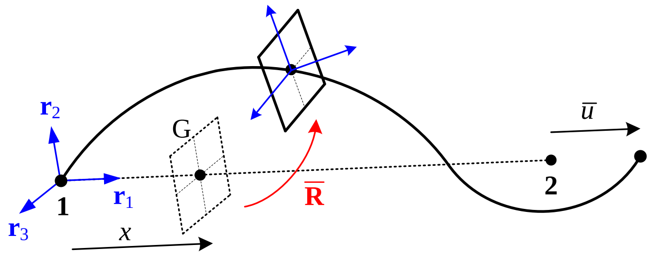

Figure 5: Local beam configuration - Rotation.

The main interest in the separation of the local deformation and the rigid body motion is that different assumptions can be made to represent the local displacements. Hence, linear interpolation is used for the axial displacement whereas cubic interpolations are used for the transverse displacements and for the axial rotation. Then, due to the particular choice of the local degrees of freedom, one has

$$\begin{bmatrix} \overline{u}_1 \\ \overline{u}_2 \\ \overline{u}_3 \\ \overline{\theta}_1 \\ \overline{\theta}_2 \\ \overline{\theta}_3 \\ \alpha \end{bmatrix} = \begin{bmatrix} N_2 & 0 & 0 & 0 & 0 & 0 & 0 & 0 & 0 \\ 0 & 0 & 0 & N_3 & 0 & 0 & N_4 & 0 & 0 \\ 0 & 0 & -N_3 & 0 & 0 & -N_4 & 0 & 0 & 0 \\ 0 & N_7 & 0 & 0 & N_8 & 0 & 0 & N_3 & N_4 \\ 0 & 0 & N_5 & 0 & 0 & N_6 & 0 & 0 & 0 \\ 0 & 0 & 0 & N_5 & 0 & 0 & N_6 & 0 & 0 \\ 0 & N_9 & 0 & 0 & -N_9 & 0 & 0 & N_5 & N_6 \end{bmatrix} \mathbf{d}_l^w \,, \tag{67}$$

where the local nodal displacement vector $\mathbf{d}_l^w$ is defined by Eq. (53).

The expressions of the interpolation functions are given by

$$\begin{aligned} &N_1 = 1 - \frac{x}{l_o}, \quad N_2 = 1 - N_1, \quad N_3 = x\left(1 - \frac{x}{l_o}\right)^2, \\ &N_4 = -\left(1 - \frac{x}{l_o}\right)\frac{x^2}{l_o}, \quad N_5 = \left(1 - \frac{3x}{l_o}\right)\left(1 - \frac{x}{l_o}\right), \quad N_6 = \left(\frac{3x}{l_o} - 2\right)\frac{x}{l_o}, \\ &N_7 = 1 - \frac{3x^2}{l_o^2} + \frac{2x^3}{l_o^3}, \quad N_8 = 1 - N_7, \quad N_9 = \frac{6x^2}{l_o^3} - \frac{6x}{l_o^2}. \end{aligned}$$

Let $\mathbf{u}_l = [0 \ \overline{u}_2 \ \overline{u}_3]^{\mathrm{T}}$ denotes the local transverse displacement vector. From Eq. (67), this vector is given by

$$\mathbf{u}_l = \mathbf{P}_1 \begin{bmatrix} \bar{\boldsymbol{\theta}}_1 \\ \bar{\boldsymbol{\theta}}_2 \end{bmatrix}, \tag{68}$$

with

$$\mathbf{P}_1 = \begin{bmatrix} 0 & 0 & 0 & 0 & 0 & 0 \\ 0 & 0 & N_3 & 0 & 0 & N_4 \\ 0 & -N_3 & 0 & 0 & -N_4 & 0 \end{bmatrix}. \tag{69}$$

From Eq. (67), the local rotation and the warping degree of freedom are given by

$$\begin{bmatrix} \bar{\boldsymbol{\theta}} \\ \alpha \end{bmatrix} = \begin{bmatrix} \mathbf{P}_2 & \mathbf{P}_3 \\ \mathbf{P}_4 & \mathbf{P}_5 \end{bmatrix} \begin{bmatrix} \bar{\boldsymbol{\theta}}_1 \\ \bar{\boldsymbol{\theta}}_2 \\ \alpha_1 \\ \alpha_2 \end{bmatrix}, \tag{70}$$

with

$$\mathbf{P}_2 = \begin{bmatrix} N_7 & 0 & 0 & N_8 & 0 & 0 \\ 0 & N_5 & 0 & 0 & N_6 & 0 \\ 0 & 0 & N_5 & 0 & 0 & N_6 \end{bmatrix}, \quad \mathbf{P}_3 = \begin{bmatrix} N_3 & N_4 \\ 0 & 0 \\ 0 & 0 \end{bmatrix}, \tag{71}$$
$$\mathbf{P}_4 = \begin{bmatrix} N_9 & 0 & 0 & -N_9 & 0 & 0 \end{bmatrix}, \quad \mathbf{P}_5 = \begin{bmatrix} N_5 & N_6 \end{bmatrix}.$$

5.2 Translational displacement variables

The position of the cross-section centroid in the global coordinate system is given by (see Fig. 4)

$$\mathrm{OG} = \mathbf{x}_\mathrm{G} = \mathbf{x}_1^g + \mathbf{u}_1^g + (x + \bar{u}_1)\,\mathbf{r}_1 + \bar{u}_2\mathbf{r}_2 + \bar{u}_3\mathbf{r}_3 . \tag{72}$$

Using Eqs. (46), (50) and (67), the above relation can be put in the following form

$$\mathrm{OG} = N_1\mathbf{x}_1^g + N_2\mathbf{x}_2^g + N_1\mathbf{u}_1^g + N_2\mathbf{u}_2^g + \mathbf{R}_r\mathbf{u}_l\,, \tag{73}$$

with $\mathbf{u}_l$ as defined in Eq. (68).

Then by taking the variation of the above equation, the following expression is obtained

$$\delta\mathrm{OG} = \delta\mathbf{u} = \mathbf{N}\,\delta\mathbf{d}_g + \mathbf{R}_r\delta\mathbf{u}_l + \delta\mathbf{R}_r\mathbf{u}_l\,, \tag{74}$$

with $\mathbf{N} = \begin{bmatrix} N_1\mathbf{I} & \mathbf{0} & N_2\mathbf{I} & \mathbf{0} \end{bmatrix}$.
One interesting property of $\mathbf{N}$ is that

$$\mathbf{N} = \mathbf{R}_r\mathbf{N}\mathbf{E}^\mathrm{T}. \tag{75}$$

The variation $\delta\mathbf{R}_r$ is calculated

$$\delta\mathbf{R}_r = \mathbf{R}_r\,\widetilde{\delta\mathbf{w}_r^e}\,. \tag{76}$$

From Eqs. (61) and (64), $\delta\mathbf{w}_r^e$ is obtained as

$$\delta\mathbf{w}_r^e = \mathbf{G}^{\mathrm{T}}\,\mathbf{E}^{\mathrm{T}}\,\delta\mathbf{d}_g\,. \tag{77}$$

By taking the differentiation of Eq. (68), one obtains

$$\delta\mathbf{u}_l = \mathbf{P}_1\begin{bmatrix}\delta\overline{\boldsymbol{\theta}}_1\\ \delta\overline{\boldsymbol{\theta}}_2\end{bmatrix}\,. \tag{78}$$

In the corotational approach, the local rotations at the nodes $\overline{\boldsymbol{\theta}}_i$ $(i=1,2)$, defined in Eq. (52), are small and the operator $\mathbf{T}_s(\overline{\boldsymbol{\theta}}_i)$ is close to the identity matrix. Consequently, see Eq. (5), the following approximation is adopted

$$\delta\overline{\mathbf{w}}_i \approx \delta\overline{\boldsymbol{\theta}}_i\,. \tag{79}$$

Then, using Eqs. (63) and (79), the expression in (78) becomes

$$\delta\mathbf{u}_l \approx \mathbf{P}_1\begin{bmatrix}\delta\overline{\mathbf{w}}_1\\ \delta\overline{\mathbf{w}}_2\end{bmatrix} = \mathbf{P}_1\,\mathbf{P}\,\mathbf{E}^{\mathrm{T}}\,\delta\mathbf{d}_g\,. \tag{80}$$

Inserting Eqs. (75) - (77) and (80) into Eq. (74), one obtains

$$\delta\mathbf{u} = \mathbf{R}_r\,\mathbf{H}_1\,\mathbf{E}^{\mathrm{T}}\,\delta\mathbf{d}_g\,, \tag{81}$$

where

$$\mathbf{H}_1 = \mathbf{N} + \mathbf{P}_1\,\mathbf{P} - \widetilde{\mathbf{u}}_l\,\mathbf{G}^{\mathrm{T}}\,. \tag{82}$$

Obviously, the translational velocity of the cross-section centroid is given as

$$\dot{\mathbf{u}} = \mathbf{R}_r\,\mathbf{H}_1\,\mathbf{E}^{\mathrm{T}}\,\dot{\mathbf{d}}_g\,. \tag{83}$$

By taking the time derivative of the above equation, the expression of the translational acceleration reads as follows

$$\ddot{\mathbf{u}} = \mathbf{R}_r\,\mathbf{H}_1\,\mathbf{E}^{\mathrm{T}}\,\ddot{\mathbf{d}}_g + \left(\dot{\mathbf{R}}_r\mathbf{H}_1\,\mathbf{E}^{\mathrm{T}} + \mathbf{R}_r\,\dot{\mathbf{H}}_1\,\mathbf{E}^{\mathrm{T}} + \mathbf{R}_r\,\mathbf{H}_1\,\dot{\mathbf{E}}^{\mathrm{T}}\right)\dot{\mathbf{d}}_g\,, \tag{84}$$

with $\dot{\mathbf{H}}_1$ given in [32].

By noting that $\dot{\mathbf{R}}_r = \mathbf{R}_r\,\widetilde{\dot{\mathbf{w}}_r^e}$ (see Eq. (76)), one has

$$\dot{\mathbf{E}} = \mathbf{E}\,\mathbf{E}_t\,,\quad \mathbf{E}_t = \begin{bmatrix}\widetilde{\dot{\mathbf{w}}_r^e} & \mathbf{0} & \mathbf{0} & \mathbf{0}\\ \mathbf{0} & \widetilde{\dot{\mathbf{w}}_r^e} & \mathbf{0} & \mathbf{0}\\ \mathbf{0} & \mathbf{0} & \widetilde{\dot{\mathbf{w}}_r^e} & \mathbf{0}\\ \mathbf{0} & \mathbf{0} & \mathbf{0} & \widetilde{\dot{\mathbf{w}}_r^e}\end{bmatrix}\,. \tag{85}$$

$\dot{\mathbf{w}}_r^e$ (see Eq. (77)) is calculated as

$$\dot{\mathbf{w}}_r^e = \mathbf{G}^{\mathrm{T}}\,\mathbf{E}^{\mathrm{T}}\,\dot{\mathbf{d}}_g\,. \tag{86}$$

By introducing the notation

$$\mathbf{C}_1 = \widetilde{\dot{\mathbf{w}}_r^e}\mathbf{H}_1 + \dot{\mathbf{H}}_1 - \mathbf{H}_1\,\mathbf{E}_t\,, \tag{87}$$

Eq. (84) can be rewritten in a more compact form as

$$\ddot{\mathbf{u}} = \mathbf{R}_r\,\mathbf{H}_1\,\mathbf{E}^{\mathrm{T}}\,\ddot{\mathbf{d}}_g + \mathbf{R}_r\,\mathbf{C}_1\,\mathbf{E}^{\mathrm{T}}\,\dot{\mathbf{d}}_g\,. \tag{88}$$

5.3 Finite rotations and warping variables

Combining Eq. (70) with the approximation defined in Eq. (79), the local spatial spin and warping variables are calculated as follows

$$\delta\overline{\mathbf{w}} = \begin{bmatrix}\mathbf{P}_2 & \mathbf{P}_3\end{bmatrix}\begin{bmatrix}\delta\overline{\mathbf{w}}_1\\ \delta\overline{\mathbf{w}}_2\\ \delta\alpha_1\\ \delta\alpha_2\end{bmatrix}, \quad \delta\alpha = \begin{bmatrix}\mathbf{P}_4 & \mathbf{P}_5\end{bmatrix}\begin{bmatrix}\delta\overline{\mathbf{w}}_1\\ \delta\overline{\mathbf{w}}_2\\ \delta\alpha_1\\ \delta\alpha_2\end{bmatrix}. \tag{89}$$

Using Eq. (63), the above equation leads to

$$\delta\overline{\mathbf{w}} = \begin{bmatrix}\mathbf{P}_2 & \mathbf{P}_3\end{bmatrix}\begin{bmatrix}\mathbf{P}\,\mathbf{E}^{\mathrm{T}} & \mathbf{0}\\ \mathbf{0} & \mathbf{I}_2\end{bmatrix}\delta\mathbf{d}_g^w = \begin{bmatrix}\mathbf{P}_2\,\mathbf{P} & \mathbf{P}_3\end{bmatrix}\mathbf{E}^{w\mathrm{T}}\,\delta\mathbf{d}_g^w, \tag{90}$$

$$\delta\alpha = \begin{bmatrix}\mathbf{P}_4 & \mathbf{P}_5\end{bmatrix}\begin{bmatrix}\mathbf{P}\,\mathbf{E}^{\mathrm{T}} & \mathbf{0}\\ \mathbf{0} & \mathbf{I}_2\end{bmatrix}\delta\mathbf{d}_g^w = \mathbf{H}_3\,\mathbf{E}^{w\mathrm{T}}\,\delta\mathbf{d}_g^w, \tag{91}$$

where

$$\mathbf{E}^w = \begin{bmatrix}\mathbf{E} & \mathbf{0}\\ \mathbf{0} & \mathbf{I}_2\end{bmatrix}, \quad \mathbf{I}_2 = \begin{bmatrix}1 & 0\\ 0 & 1\end{bmatrix}, \quad \mathbf{H}_3 = \begin{bmatrix}\mathbf{P}_4\,\mathbf{P} & \mathbf{P}_5\end{bmatrix}. \tag{92}$$

Using Eqs. (58) and (59), the spatial spin variables, associated to the global rotation of a cross-section, are evaluated using

$$\delta\mathbf{w} = \mathbf{R}_r\delta\mathbf{w}^e = \mathbf{R}_r\left(\delta\mathbf{w}_r^e + \delta\overline{\mathbf{w}}\right). \tag{93}$$

Using Eqs. (77) and (90), the above expression can be rewritten in as

$$\delta\mathbf{w} = \mathbf{R}_r\,\mathbf{H}_2\,\mathbf{E}^{w\mathrm{T}}\,\delta\mathbf{d}_g^w, \tag{94}$$

with

$$\mathbf{H}_2 = \begin{bmatrix}\mathbf{P}_2\,\mathbf{P} + \mathbf{G}^{\mathrm{T}} & \mathbf{P}_3\end{bmatrix}. \tag{95}$$

$\dot{\mathbf{w}}$ and $\dot{\alpha}$ are calculated with expressions similar to (91) and (94)

$$\dot{\mathbf{w}} = \mathbf{R}_r\,\mathbf{H}_2\,\mathbf{E}^{w\mathrm{T}}\,\dot{\mathbf{d}}_g^w, \quad \dot{\alpha} = \mathbf{H}_3\,\mathbf{E}^{w\mathrm{T}}\,\dot{\mathbf{d}}_g^w. \tag{96}$$

$\ddot{\mathbf{w}}$ is obtained by taking the time derivative of $\dot{\mathbf{w}}$

$$\ddot{\mathbf{w}} = \mathbf{R}_r\,\mathbf{H}_2\,\mathbf{E}^{w\mathrm{T}}\,\ddot{\mathbf{d}}_g^w + \mathbf{R}_r\left(\widetilde{\dot{\mathbf{w}}_r^e}\,\mathbf{H}_2 + \dot{\mathbf{H}}_2 - \mathbf{H}_2\,\mathbf{E}_t^w\right)\mathbf{E}^{w\mathrm{T}}\,\dot{\mathbf{d}}_g^w, \tag{97}$$

with $\dot{\mathbf{H}}_2$ given in [32]

$$\mathbf{E}_t^w = \begin{bmatrix}\mathbf{E}_t & \mathbf{0}\\ \mathbf{0} & \mathbf{0}_2\end{bmatrix}. \tag{98}$$

By noting that

$$\mathbf{P}_4\,\mathbf{P} = \begin{bmatrix} 0 & 0 & 0 & N_9 & 0 & 0 & 0 & 0 & 0 & -N_9 & 0 & 0 \end{bmatrix}, \tag{99}$$

and by taking the time derivative of $\dot{\alpha}$, the expression of $\ddot{\alpha}$ is obtained

$$\ddot{\alpha} = \mathbf{H}_3\,\mathbf{E}^{w\mathrm{T}}\,\ddot{\mathbf{d}}_g^w - \mathbf{H}_3\,\mathbf{E}_t^w\,\mathbf{E}^{w\mathrm{T}}\,\dot{\mathbf{d}}_g^w\,. \tag{100}$$

Introducing Eqs. (91),(94),(96),(97), and (100) into Eq. (42), one obtains

$$\delta\mathbf{w}^w = \begin{bmatrix} \mathbf{R}_r & \mathbf{0} \\ \mathbf{0} & 1 \end{bmatrix} \begin{bmatrix} \mathbf{H}_2 \\ \mathbf{H}_3 \end{bmatrix} \mathbf{E}^{w\mathrm{T}}\,\delta\mathbf{d}_g^w = \mathbf{R}_r^w\,\mathbf{H}_2^w\,\mathbf{E}^{w\mathrm{T}}\,\delta\mathbf{d}_g^w\,, \tag{101}$$

$$\dot{\mathbf{w}}^w = \mathbf{R}_r^w\,\mathbf{H}_2^w\,\mathbf{E}^{w\mathrm{T}}\,\dot{\mathbf{d}}_g^w\,, \tag{102}$$

$$\ddot{\mathbf{w}}^w = \mathbf{R}_r^w\,\mathbf{H}_2^w\,\mathbf{E}^{w\mathrm{T}}\,\ddot{\mathbf{d}}_g^w + \mathbf{R}_r^w\,\mathbf{C}_2\,\mathbf{E}^{w\mathrm{T}}\,\dot{\mathbf{d}}_g^w\,, \tag{103}$$

where

$$\mathbf{C}_2 = \begin{bmatrix} \widetilde{\dot{\mathbf{w}}_r^e}\,\mathbf{H}_2 + \dot{\mathbf{H}}_2 - \mathbf{H}_2\,\mathbf{E}_t^w \\ -\mathbf{H}_3\,\mathbf{E}_t^w \end{bmatrix}. \tag{104}$$

5.4 Inertia force vector and tangent dynamic matrix

By inserting the expressions of $\delta\mathbf{u}$ and $\delta\mathbf{w}^w$ given in Eqs. (81) and (101) into Eq. (44), the inertia force vector is obtained as

$$\mathbf{f}_\mathrm{k}^w = \mathbf{E}^w \left\{ \begin{bmatrix} \int_{l_o} \mathbf{H}_1^\mathrm{T}\,\mathbf{R}_r^\mathrm{T}\,A_\rho\,\ddot{\mathbf{u}}\mathrm{d}l \\ \mathbf{0} \end{bmatrix} + \int_{l_o} \mathbf{H}_2^{w\mathrm{T}}\,\mathbf{R}_r^{w\mathrm{T}} \left[\mathbf{I}_\rho^1\,\ddot{\mathbf{w}}^w + \mathbf{I}_\rho^2\,\dot{\mathbf{w}}^w \right] \mathrm{d}l \right\}. \tag{105}$$

As shown in the above equation, the inertia force vector depends on $\mathbf{d}_g^w, \dot{\mathbf{d}}_g^w$ and $\ddot{\mathbf{d}}_g^w$. Hence, linearization of this force vector is evaluated as follows

$$\Delta\mathbf{f}_\mathrm{k}^w = \mathbf{M}\Delta\ddot{\mathbf{d}}_g^w + \mathbf{C}_\mathrm{k}\Delta\dot{\mathbf{d}}_g^w + \mathbf{K}_\mathrm{k}\Delta\mathbf{d}_g^w\,. \tag{106}$$

Some authors [8, 18] proposed to keep only the mass matrix $\mathbf{M}$, and to eliminate the gyroscopic $\mathbf{C}_\mathrm{k}$ and centrifugal $\mathbf{K}_\mathrm{k}$ dynamic matrices. However, in [30], extensive numerical studies have shown that it is advantageous to retain also the gyroscopic matrix as it enhances the computational efficiency. The same approach is used here. The centrifugal matrix, whose derivation is complicated and would give rise to a lengthy mathematical expression, is neglected. Therefore, the iterative scheme of the present formulation is implemented with the following approximative linearization

$$\Delta\mathbf{f}_\mathrm{k}^w \approx \mathbf{M}\Delta\ddot{\mathbf{d}}_g^w + \mathbf{C}_\mathrm{k}\Delta\dot{\mathbf{d}}_g^w\,. \tag{107}$$

From the expressions (88), (102) and (103), the following linearizations are derived

$$\begin{aligned}\Delta\ddot{\mathbf{u}} &= \mathbf{R}_r\left[\mathbf{H}_1\,\mathbf{E}^{\mathrm{T}}\,\Delta\ddot{\mathbf{d}}_g + \mathbf{C}_1\,\mathbf{E}^{\mathrm{T}}\,\Delta\dot{\mathbf{d}}_g + (\frac{\partial \mathbf{C}_1}{\partial \dot{\mathbf{d}}_g}\Delta\dot{\mathbf{d}}_g)\,\mathbf{E}^{\mathrm{T}}\,\dot{\mathbf{d}}_g\right] + f(\Delta\mathbf{d}_g)\\ &= \mathbf{R}_r\left[\mathbf{H}_1\,\mathbf{E}^{\mathrm{T}}\,\Delta\ddot{\mathbf{d}}_g + (\mathbf{C}_1+\mathbf{C}_3)\,\mathbf{E}^{\mathrm{T}}\,\Delta\dot{\mathbf{d}}_g\right] + f(\Delta\mathbf{d}_g)\,,\end{aligned} \tag{108}$$

$$\Delta\dot{\mathbf{w}}^w = \mathbf{R}_r^w\,\mathbf{H}_2^w\,\mathbf{E}^{w\mathrm{T}}\,\Delta\dot{\mathbf{d}}_g^w + f(\Delta\mathbf{d}_g^w)\,, \tag{109}$$

$$\begin{aligned}\Delta\ddot{\mathbf{w}}^w &= \mathbf{R}_r^w\left[\mathbf{H}_2^w\,\mathbf{E}^{w\mathrm{T}}\,\Delta\ddot{\mathbf{d}}_g^w + \mathbf{C}_2\,\mathbf{E}^{w\mathrm{T}}\,\Delta\dot{\mathbf{d}}_g^w + (\frac{\partial \mathbf{C}_2}{\partial \dot{\mathbf{d}}_g^w}\Delta\dot{\mathbf{d}}_g^w)\,\mathbf{E}^{w\mathrm{T}}\,\dot{\mathbf{d}}_g^w\right] + f(\Delta\mathbf{d}_g^w)\\ &= \mathbf{R}_r^w\left[\mathbf{H}_2^w\,\mathbf{E}^{w\mathrm{T}}\,\Delta\ddot{\mathbf{d}}_g^w + (\mathbf{C}_2+\mathbf{C}_4)\,\mathbf{E}^{w\mathrm{T}}\,\Delta\dot{\mathbf{d}}_g^w\right] + f(\Delta\mathbf{d}_g^w)\,,\end{aligned} \tag{110}$$

with $\mathbf{C}_3$ and $\mathbf{C}_4$ given [32].

Using the above linearizations, the expression of the mass matrix $\mathbf{M}$ is obtained as

$$\begin{aligned}\mathbf{M} &= \mathbf{E}^w\left\{\begin{bmatrix}\int_{l_o}\mathbf{H}_1^{\mathrm{T}}A_\rho\,\mathbf{H}_1\,\mathrm{d}l & \mathbf{0}\\ \mathbf{0} & \mathbf{0}\end{bmatrix} + \int_{l_o}\mathbf{H}_2^{w\mathrm{T}}\,\mathbf{R}_r^{w\mathrm{T}}\,\mathbf{I}_\rho^1\,\mathbf{R}_r^w\,\mathbf{H}_2^w\,\mathrm{d}l\right\}\mathbf{E}^{w\mathrm{T}}\\ &= \mathbf{E}^w\,\mathbf{M}^e\,\mathbf{E}^{w\mathrm{T}}\,.\end{aligned} \tag{111}$$

Regarding the gyroscopic matrix $\mathbf{C}_\mathrm{k}$, the following intermediate variation is used

$$\begin{aligned}\frac{\partial \mathbf{I}_\rho^2\,\dot{\mathbf{w}}^w}{\partial \dot{\mathbf{w}}^w}\Delta\dot{\mathbf{w}}^w &= \begin{bmatrix}\widetilde{\dot{\mathbf{w}}}\,(\mathbf{I}_\rho+\mathbf{I}_\alpha)\Delta\dot{\mathbf{w}} + \widetilde{\Delta\dot{\mathbf{w}}}\,(\mathbf{I}_\rho+\mathbf{I}_\alpha)\dot{\mathbf{w}} + \mathbf{I}_c\,(\Delta\dot{\mathbf{w}}\,\dot{\alpha} + \dot{\mathbf{w}}\,\Delta\dot{\alpha})\\ -\Delta\dot{\mathbf{w}}^{\mathrm{T}}\,\mathbf{I}_\alpha'\,\dot{\mathbf{w}} - \dot{\mathbf{w}}^{\mathrm{T}}\,\mathbf{I}_\alpha'\,\Delta\dot{\mathbf{w}}\end{bmatrix}\\ &= \begin{bmatrix}\widetilde{\dot{\mathbf{w}}}\,(\mathbf{I}_\rho+\mathbf{I}_\alpha) & \mathbf{I}_c\,\dot{\mathbf{w}}\\ -\dot{\mathbf{w}}^{\mathrm{T}}\,\mathbf{I}_\alpha' & 0\end{bmatrix}\Delta\dot{\mathbf{w}}^w + \begin{bmatrix}\widetilde{(\mathbf{I}_\rho+\mathbf{I}_\alpha)\dot{\mathbf{w}}} + \mathbf{I}_c\,\dot{\alpha} & \mathbf{0}\\ -\dot{\mathbf{w}}^{\mathrm{T}}\,\mathbf{I}_\alpha'^{\mathrm{T}} & 0\end{bmatrix}\Delta\dot{\mathbf{w}}^w\\ &= \left(\mathbf{I}_\rho^2+\mathbf{I}_\rho^3\right)\Delta\dot{\mathbf{w}}^w\,.\end{aligned} \tag{112}$$

Finally, the gyroscopic matrix $\mathbf{C}_\mathrm{k}$ is calculated from

$$\begin{aligned}\mathbf{C}_\mathrm{k} = \mathbf{E}^w&\left\{\begin{bmatrix}\int_{l_o}\mathbf{H}_1^{\mathrm{T}}A_\rho\,(\mathbf{C}_1+\mathbf{C}_3)\,\mathrm{d}l & \mathbf{0}\\ \mathbf{0} & \mathbf{0}\end{bmatrix} + \int_{l_o}\mathbf{H}_2^{w\mathrm{T}}\,\mathbf{R}_r^{w\mathrm{T}}\,\mathbf{I}_\rho^1\,\mathbf{R}_r^w\,(\mathbf{C}_2+\mathbf{C}_4)\,\mathrm{d}l\right.\\ &\left.+\int_{l_o}\mathbf{H}_2^{w\mathrm{T}}\,\mathbf{R}_r^{w\mathrm{T}}\left(\mathbf{I}_\rho^2+\mathbf{I}_\rho^3\right)\mathbf{R}_r^w\,\mathbf{H}_2^w\,\mathrm{d}l\right\}\mathbf{E}^{w\mathrm{T}} = \mathbf{E}^w\,\mathbf{C}_\mathrm{k}^e\,\mathbf{E}^{w\mathrm{T}}\,.\end{aligned} \tag{113}$$

In this work, the warping deformations and the eccentricity of the shear center have been taken into account in deriving the inertial terms, see Eq. (13). Consequently, several additional terms have been introduced in the expressions of the inertia force vector and the tangent (mass and gyroscopic) matrices. The importance of these terms can be discussed. In the five numerical examples presented in Section 7, it has been found, as expected, that the warping deformations in the dynamic terms have a negligible contribution to the response and can be omitted. This is done by setting $I_\omega = 0$ in Eqs. (19) and (20).

The eccentricity of the shear center with respect to the centroid generates extra dynamic terms whose importance has been investigated. It appears that for slender beams (Examples 7.1), these terms do not affect the results and can be therefore neglected. But as it has bee shown in [32], they may have a significant contribution for short beams.

If $I_\omega = y_c = z_c = 0$ is adopted, then the expression of the inertia force vector in Eq. (105) can be simplified as

$$\mathbf{f}_{\mathrm{k}}^{w} = \mathbf{E}^{w} \left\{ \begin{bmatrix} \int_{l_o} \mathbf{H}_1^{\mathrm{T}} \mathbf{R}_r^{\mathrm{T}} A_\rho \ddot{\mathbf{u}} \mathrm{d}l \\ \mathbf{0} \end{bmatrix} + \int_{l_o} \mathbf{H}_2^{\mathrm{T}} \mathbf{R}_r^{\mathrm{T}} \left[\mathbf{I}_\rho \ddot{\mathbf{w}} + \widetilde{\dot{\mathbf{w}}} \mathbf{I}_\rho \dot{\mathbf{w}} \right] \mathrm{d}l \right\}, \tag{114}$$

and similar simplifications apply also for the expressions of the mass and gyroscopic matrices.

6 Internal force vector and tangent stiffness matrix

The purpose of this section is to present briefly the derivation of the inertial force vector and the tangent stiffness matrix. A complete description can be found in [5].

The local nodal displacements and rotations defined in Eq. (53) are extracted from the global degrees of freedom using Eqs. (50), (51) and (52).

The local internal force vector $\mathbf{f}_{\mathrm{l}}^{w}$ and the local tangent stiffness matrix $\mathbf{K}_{\mathrm{l}}^{w}$ associated with $\delta \mathbf{d}_l^{w}$ (see Eq. (54)) are derived using the same local beam kinematic description as in 5.1. However, to incorporate the bending shear deformations, the Hermitian shape functions for the transverse displacements are slightly modified as suggested in the Interdependent Interpolation Element (IIE) [39]. The Maple codes for $\mathbf{f}_{\mathrm{l}}^{w}$ and $\mathbf{K}_{\mathrm{l}}^{w}$ are given [32]. A low order of geometrical nonlinearity is introduced through a shallow arch strain description and the Wagner term.

The global internal force vector $\mathbf{f}_{\mathrm{g}}^{w}$ and the global tangent stiffness matrix $\mathbf{K}_{\mathrm{g}}^{w}$ associated with $\delta \mathbf{d}_g^{w}$ (see Eq. (55)) are obtained through a change of variables based on the transformation matrix $\mathbf{B}^{w}$ defined by

$$\delta \mathbf{d}_l^{w} = \mathbf{B}^{w} \, \delta \mathbf{d}_g^{w}. \tag{115}$$

By equating the internal virtual work in both the global and local systems, the expression of the global internal force vector $\mathbf{f}_{\mathrm{g}}^{w}$ is obtained as

$$\mathbf{f}_{\mathrm{g}}^{w} = \mathbf{B}^{w\mathrm{T}} \mathbf{f}_{\mathrm{l}}^{w}. \tag{116}$$

By taking the variations of Eq. (116), the expression of the global tangent stiffness matrix $\mathbf{K}_{\mathrm{g}}^{w}$ is obtained

$$\mathbf{K}_{\mathrm{g}}^{w} = \mathbf{B}^{w\mathrm{T}} \mathbf{K}_{\mathrm{l}}^{w} \mathbf{B}^{w} + \left. \frac{\partial (\mathbf{B}^{w\mathrm{T}} \mathbf{f}_{\mathrm{l}}^{w})}{\partial \mathbf{d}_g^{w}} \right|_{\mathbf{f}_{\mathrm{l}}^{w}}. \tag{117}$$

The expressions of $\mathbf{f}_{\mathrm{g}}^{w}$ and $\mathbf{K}_{\mathrm{g}}^{w}$ are given in [5].

7 NUMERICAL EXAMPLE

The purpose of the five numerical examples presented in this section is to assess the accuracy of the proposed corotational dynamic formulation for beam with thin-walled cross-section. For that, additional 3D-solid analyses are performed with the commercial finite element program Abaqus.

Besides, the influence of the warping deformations (I_ω) and the shear center eccentricity (y_c, z_c) in the dynamic terms of the corotational formulation is also studied. In all the examples, and as expected, the same results have been obtained with and without I_ω in the inertia terms. In Example which consists of a slender beams, the same results have been obtained with $y_c = z_c = 0$. However, for the short beam (see [32], different results are obtained with and without account for the eccentricity of the shear center.

Regarding the time integration method, the HHT α method with $\alpha = -0.05$ is used in this work. This energy-dissipative method, which is implemented in several commercial FEM programs (Abaqus, Lusas) and was employed by many authors [8, 11, 27], limits the influence of high frequencies by introducing a numerical damping. However, a numerical damping gives also a dissipation of the total energy, which can affect long time analyses. It can be noted that for beam structures, more robust alternatives to the HHT α method have been proposed in the literature [23].

In the present work, at the beginning of each time step, the predictor proposed by Crisfield [12] for the particular case of linear inertia force vector and further developed for the general case by the authors [30], is adopted. The idea of this predictor is to use the tangent operator at the time instant t_n to predict the values at the time instant t_{n+1}.

Damping is not considered. The following convergence criterion is adopted: the norm of the residual vector must be less than the prescribed tolerance $\varepsilon_f = 10^{-5}$.

The following material properties are used for all the five examples: $E = 210$ GPa, $\nu = 0.33$ and $\rho = 7850$ kg/m^3. All the dimensions in the figures are in meter.

7.1 Example: Cantilever beam with a T cross-section

The nonlinear dynamic behavior of a cantilever beam with a T cross-section, see Fig. 6, is investigated. The eccentricity of the shear center is $y_c = 0.046$ m. At the left end, the beam is clamped and all degrees of freedom, including warping, are set to zero. At the point O of the right end section, two time-varying loads are applied: $F_y^{\mathrm{O}} = -50F$, $F_z^{\mathrm{O}} = 25F$. The time evolution of F is given in Fig. 7.

The cantilever is modeled using 40 corotational beam elements. Besides, the commercial finite element software Abaqus is employed considering both beam and 3D-solid elements.

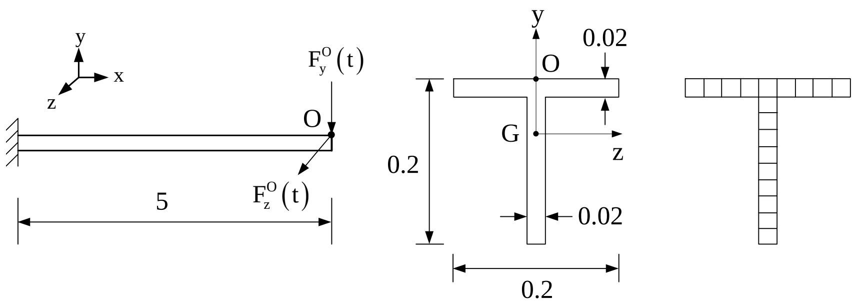

Figure 6: Cantilever beam with T cross-section : geometrical data.

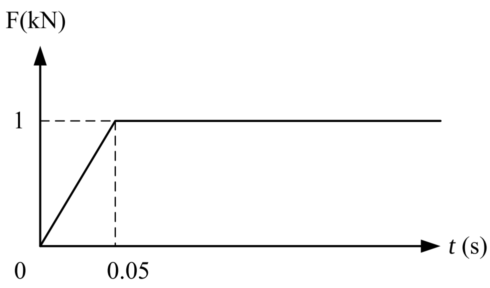

Figure 7: Cantilever beam with T cross-section - Loading history.

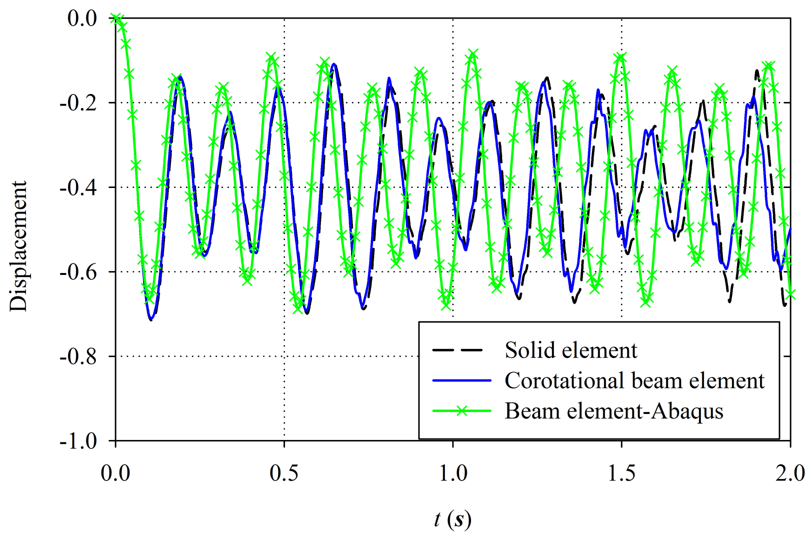

Figure 8: Cantilever beam with T cross-section - Time evolution of the displacement u_y of point G.

For the beam analysis, 80 B31OS elements are used. The beam element B31OS has seven degrees of freedom at each node. The additional degree of freedom represents the warping of the beam cross-section. Linear interpolations are used for all variables. For the 3D-solid analysis, the mesh consists of $18 \cdot 160 = 2880$ isoparametric 20 node elements (see Fig. 6). All analyses are performed with a time step $\Delta t = 10^{-3}$ s.

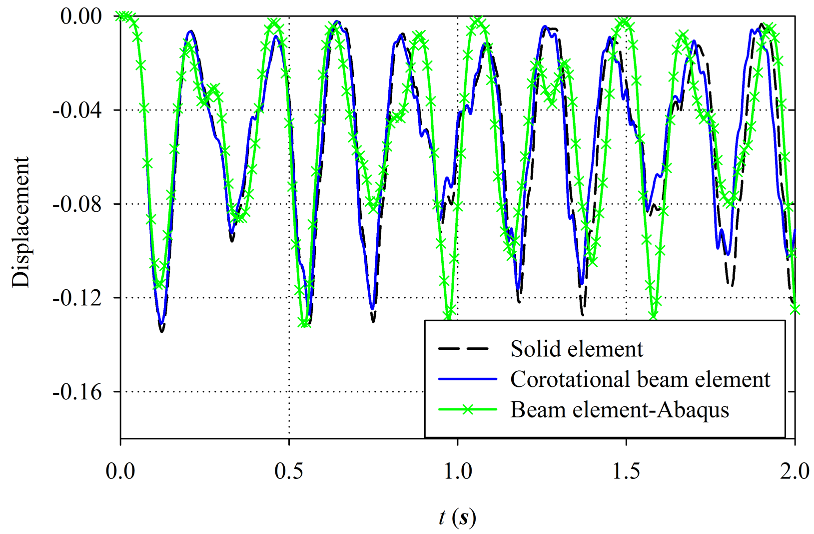

Figure 9: Cantilever beam with T cross-section - Time evolution of the displacement u_x of point G.

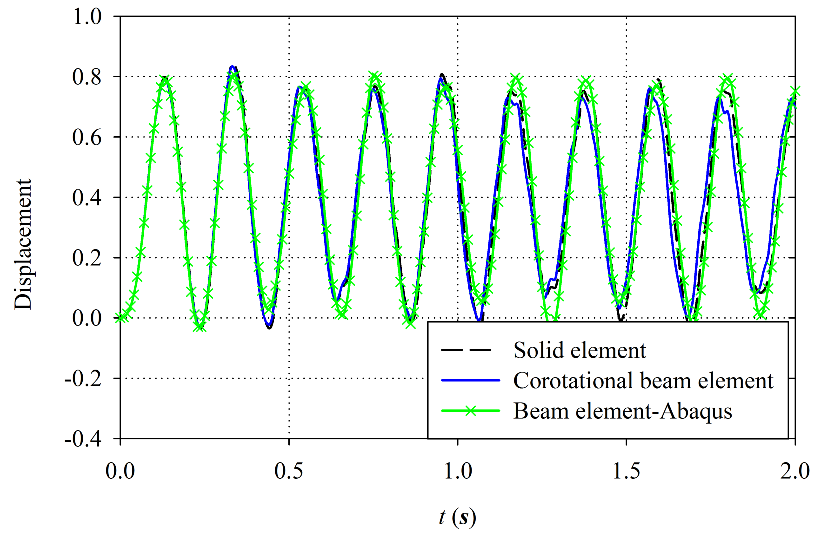

Figure 10: Cantilever beam with T cross-section - Time evolution of the displacement u_z of point G.

The displacements of the right end centroid G are depicted in Figs. 8, 9, and 10. A very good agreement in the predictions of both the corotational beam element and Abaqus 3D-solid analyses is obtained. However, large discrepancies in the predictions of both Abaqus beam and 3D-solid models can be observed, especially in Fig. 8.

A small but increasing phase lead can be observed between the results obtained with the corotational beam element and those obtained with the solid analysis. To investigate this aspect, the problem has been run for a time period of 7 s. The results are shown in Fig. 11. It can be observed that after 7 s the phase lead remains negligible. In fact, this increasing phase lead is due to a small difference in the estimation of natural frequencies between the two models.

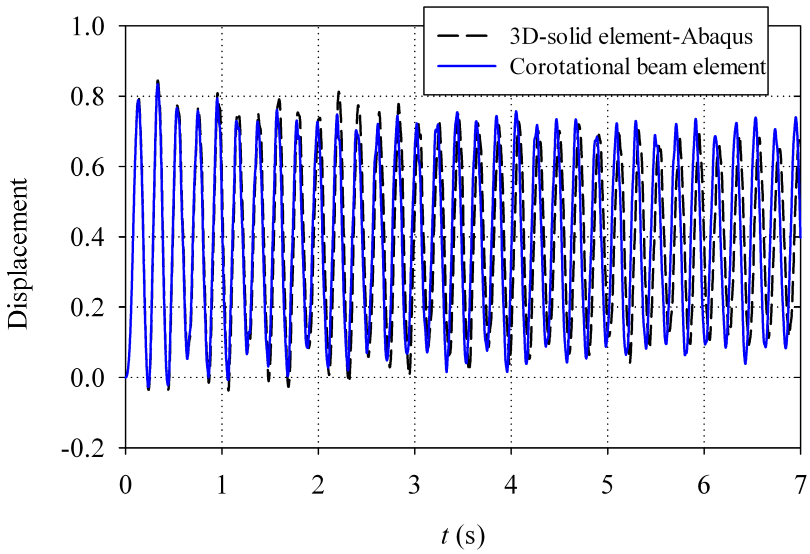

Figure 11: Cantilever beam with T cross-section - Time evolution of the displacement u_z of point G for 7 s.

8 CONCLUSIONS

In this paper, a corotational dynamic formulation for nonlinear analysis of beams with arbitrary thin-walled cross-sections was developed. The formulation is an extension of the one proposed by the authors in [31]. The same kinematic assumptions were used to derive the static and dynamic terms. Hence, the element has seven degrees of freedom at each node and cubic shape functions are used to interpolate local transverse displacements and axial rotations.

The warping deformations and the shear center eccentricity were fully taken into account in the derivation of the dynamic terms. This leads to additional terms in the expressions of the inertia force vector and the tangent (mass and gyroscopic) dynamic matrices.

A very good agreement between the results obtained with the corotational beam element and the 3D-solid element was obtained. Besides, the numerical results also showed that the warping deformations have a negligible influence in the dynamic terms and could be omitted. As shown in [32] However, the additional dynamic terms due to the shear center eccentricity cannot always be neglected.

REFERENCES

[1] R. Grutmann, R. Sauer, W. Wagner, Theory and numerics of three-dimensional beams with elastoplastic behaviour, Int. J. Num. Methods. Engrg., Vol. 48, 1675-1702 (2000).

[2] J. Argyris, An excursion into large rotations, Comput. Methods Appl. Mech. Engrg., Vol. 32, 85-155 (1982).

[3] R. Alsafadie, J.-M. Battini, M. Hjiaj, H. Somja, A comparative study of displacement and mixed-based corotational finite element formulations for elasto-plastic three-dimensional beam analysis, Engerg. Computs., Vol. 28, 7, 939-982 (2011).

[4] K.J. Bathe, E. Ramm, Wilson E.L., Finite element formulations for large deformation dynamic analysis, Int. J. Num. Methods. Engrg., Vol. 9, 353-386 (1975).

[5] J.-M. Battini, C. Pacoste, Co-rotational beam elements with warping effects in instability problems, Comput. Methods Appl. Mech. Engrg., Vol. 191, 1755-1789 (2002).

[6] K. Behdinan, M.C Stylianou, B. Tabarrok, Co-rotational dynamic analysis of flexible beams, Comput. Methods Appl. Mech. Engrg., Vol. 154, 151-161 (1998).

[7] P. Betsch, P. Steinmann, Constrained dynamics of geometrically exact beams, Comput. Mech., Vol. 31, 49-59 (2003).

[8] A. Cardona, M. Geradin, A beam finite element non-linear theory with finite rotations, Int. J. Num. Methods. Engrg., Vol. 26, 2403-2438 (1988).

[9] M.A. Crisfield, J. Shi, An energy conserving co-rotational procedure for non-linear dynamics with finite elements, Nonlinear Dynamics, Vol. 9, 37-52 (1996).

[10] M.A. Crisfield, G.F. Moita, A unified co-rotational framework for solids shells and beams, Int. J. Solids Struct., Vol. 33, 29692992 (1996).

[11] M.A. Crisfield, U. Galvanetto, G. Jelenić, Dynamics of 3-D co-rotational beams, Comput. Mech., Vol. 20, 507-519 (1997).

[12] M.A. Crisfield, Non-Linear Finite Element Analysis of Solids and Structures, Volume 2: Advanced Topics, Wiley, Chischester (1997).

[13] H.A. Elkaranshawy, M.A. Dokainish, Corotational finite element analysis of planar flexible multibody systems, Comput. Struct., Vol. 54, No.5, 881-890 (1995).

[14] U. Galvanetto, M.A. Crisfield, An energy conserving co-rotational procedure for dynamics of planar beam structures, Int. J. Num. Methods. Engrg., Vol. 39, 2265-2282 (1996).

[15] M. Geradin, A. Cardona, Kinematics and dynamics of rigid and flexible mechanisms using finite elements and quaternion algebra, Comput. Mech., Vol. 4, 115-135 (1989).

[16] M. Geradin, A. Cardona, Flexible multibody dynamics : A finite element approach, 120-127. Wiley, Chischester (2001).

[17] K.M. Hsiao, R.T. Yang, A co-rotational formulation for nonlinear dynamic analysis of curved Euler beam, Comput. Struct. , Vol. 54, No.6, 1091-1097 (1995).

[18] K.M. Hsiao, J.Y. Lin, W.Y. Lin, A consistent co-rotational finite element formulation for geometrically nonlinear dynamics analysis of 3-D beams, Comput. Methods Appl. Mech. Engrg., Vol. 169, 1-18 (1999).

[19] K.M. Hsiao, W.Y. Lin, R.H. Chen, Geometrically non-linear dynamic analysis of thin-walled beams, Proc. World Congress Engrg., Vol. II (2009).

[20] A. Ibrahimbegović, F. Frey, I. Kožar, Computational aspects of vector-like parameterization of three-dimensional finite rotations, Int. J. Num. Methods. Engrg., Vol. 38, 3653-3673 (1995).

[21] A. Ibrahimbegović, On the choice of finite rotation parameters, Comput. Methods Appl. Mech. Engrg., Vol. 149, 49-71 (1997).

[22] A. Ibrahimbegović, M.A. Mikdad, Finite rotations in dynamics of beams and implicit time-stepping schemes, Int. J. Num. Methods. Engrg., Vol. 41, 781-814 (1998).

[23] A. Ibrahimbegović, S. Mamouri, Energy conserving/decaying implicit time-stepping scheme for nonlinear dynamics of three-dimensional beams undergoing finite rotations, Comput. Methods Appl. Mech. Engrg., Vol. 191, 4241-4258 (2002).

[24] M. Iura, S.N. Atluri, Dynamic analysis of finitely stretched and rotated three-dimensional space-curved beams, Comput. Struct., Vol. 29, 875-889 (1988).

[25] M. Iura, S.N. Atluri, Dynamic analysis of planar flexible beams with finite rotations by using inertial and rotating frames, Comput. Struct., Vol. 55, No.3, 453-462 (1995).

[26] G. Jelenić, M.A. Crisfield, Interpolation of rotational variables in nonlinear dynamics of 3D beams, Int. J. Num. Methods. Engrg., Vol. 43, 1193-1222 (1998).

[27] G. Jelenić, M.A. Crisfield, Geometrically exact 3D beam theory: implementation of a strain-invariant element for stactics and dynamics, Comput. Methods Appl. Mech. Engrg., Vol. 171, 141-171 (1999).

[28] S. Krenk, Non-Linear Modeling And Analysis Of Solids And Structures, 47-75, Cambridge University Press, New York (2009).

[29] T.-N. Le, J.-M. Battini, M. Hjiaj, Efficient formulation for dynamics of corotational 2D beams, Comput. Mech., Vol. 48, No. 2, 153-161 (2011).

[30] T.-N. Le, J.-M. Battini, M. Hjiaj, Dynamics of 3D beam elements in a corotational context: A comparative study of established and new formulations, Finite Elem. Anal. Des., Vol. 61, 97-111 (2012).

[31] T.-N. Le, J.-M. Battini, M. Hjiaj, A consistent 3D corotational beam element for nonlinear dynamic analysis of flexible structures, Comput. Methods Appl. Mech. Engrg., 2vol. 269: 538-565. (2014).

[32] T.-N. Le, J.-M. Battini, M. Hjiaj, Corotational formulation for nonlinear dynamics of beams with arbitrary thin-walled cross-sections, Computers and Structures, vol.134: 112-127 (2014).

[33] E.V. Lens, A. Cardona, A nonlinear beam element formulation in the framework of an energy preserving time integration scheme for constrained multibody systems dynamics, Comput. Struct. , Vol. 86, 47-63 (2008).

[34] J. Mäkinen, Total Lagrangian Reissner's geometrically exact beam element without singularities, Int. J. Num. Methods. Engrg., Vol. 70, 1009-1048 (2007).

[35] N. Masuda, T. Nishiwaki, M. Minaaawa, Nonlinear dynamic analysis of frame structures, Comput. Struct., Vol. 27, No.1, 103-110 (1987).

[36] B. Nour-Omid, C.C. Rankin, Finite rotation analysis and consistent linearization using projectors, Comput. Methods Appl. Mech. Engrg., Vol. 93, 353-384 1991.

[37] C. Oran, A. Kassimali, Large deformations of framed structures under static and dynamic loads, Comput. Struct., Vol. 6, 539-547 (1976).

[38] C.C. Rankin, B. Nour-Omid, The use of projectors to improve finite element performance, Comput. Struct., Vol. 30, 257-267 (1988).

[39] J.N. Reddy, On locking-free shear deformable beam finite elements, Comput. Methods Appl. Mech. Engrg., Vol. 149, 113-132 (1997).

[40] J.C. Simo, L. Vu-Quoc, On the dynamics in space of rods undergoing large motions - A geometrically exact approach, Comput. Methods Appl. Mech. Engrg., Vol. 66, 125-161 (1988).

[41] Q. Xue, J.L Meek, Dynamic response and instability of frame structures, Comput. Methods Appl. Mech. Engrg., Vol. 190, 5233-5242 (2001).

[42] E. Zupan, M. Saje, D. Zupan, Quaternion-based dynamics of geometrically nonlinear spatial beams using the RungeKutta method, Finite Elem. Anal. Des., Vol. 54, 48-60 (2012).

[43] E. Zupan, M. Saje, D. Zupan, Dynamics of spatial beams in quaternion description based on the Newmark integration scheme, Comput. Mech., Vol. 51, 47-64 (2013).